High-pressure lattice dynamics and thermoelasticity of MgO

B. B. Karki and R. M. Wentzcovitch*

Department of Chemical Engineering and Materials Science, Minnesota Supercomputing Institute, University of Minnesota, Minneapolis, Minnesota 55455

S. de Gironcoli and S. Baroni

Scuola Internazionale Superiore di Studi Avanzati (SISSA), Instituto Nazionale Fisica della Materia (INFM), I-34014 Trieste, Italy
(Received 14 October 1999)

We present an *ab initio* study of the thermoelastic properties of MgO over a wide range of pressure and temperature. Phonon dispersions for equilibrium and strained configurations are obtained from density-functional perturbation theory. They are used to calculate thermodynamical potentials within the quasiharmonic approximation and several derived quantities of physical interest without further approximations. These include the temperature dependence of individual elastic constants at high pressures. Extensive and successful comparisons with experimental data demonstrate that the quasiharmonic approximation combined with *ab initio* phonon calculations provides an important theoretical approach for exploring thermodynamical properties of materials over a considerable pressure-temperature regime.

I. INTRODUCTION

The high-pressure high-temperature behavior of MgO has long been a subject of great interest for experimental and theoretical investigations for several reasons. MgO is often regarded as a prototype oxide due to its structural simplicity and wide pressure-temperature stability field. It is an important component of Earth's lower mantle (660 to 2890 km depth) existing as magnesiowüstite—(Mg,Fe)O. In addition, it is also useful as a pressure standard in x-ray diffraction experiments and as an industrial ceramic.

Lattice vibrations account for a number of macroscopic properties of solids such as thermal expansion, specific heat, and entropy. They can also be used to study the temperature dependence of elastic moduli. Propagation of elastic waves in a medium and their dependence on direction can be investigated from knowledge of the single crystal elastic constants. Particularly, the high-pressure (P) and high-temperature (T) behavior of the elastic wave velocities and anisotropy of geophysically relevant phases like MgO are of immediate significance in interpreting seismological observations of Earth's deep interior. Lattice dynamics and elasticity, as they are governed by interatomic forces, can be expected to provide significant indication of changes in structure and nature of bonding induced by pressure and temperature.

Experiments have shown that MgO is stable in the B1 phase up to at least 227 GPa,[1] consistent with theoretical predictions.[2–8] While its phase stability and equation of state are widely studied by experiments,[1,9–11] measurements of vibrational and elastic properties of MgO are limited. Its vibrational spectrum at ambient conditions is well known.[12] Pressure dependence of six vibrational modes has been measured by using the sideband fluorescence method.[13] The latest measurements of single-crystal elastic constants at simultaneous $P-T$ conditions are limited to 8 GPa and 1600 K (Ref. 14) whereas the elasticity data have been obtained up to ~19 GPa at ambient temperature[15] and up to 1800 K at ambient pressure.[16]

Several theoretical methods have been applied to MgO; several of these studies were based on semiempirical or simplified nonempirical models (e.g., potential-induced breathing model).[5–7] Lattice dynamics of MgO has been studied from first principles only at zero pressure[17] although its elasticity has been determined at high pressure.[8] Here, we report the phonon dispersions of MgO as a function of pressure obtained by linear-response calculations within the framework of density functional perturbation theory.[18] Using them we have recently studied the cross pressure-temperature variations of elastic constants.[19] In this paper, several other thermodynamic quantities of interest such as thermal expansivity, heat capacity, and entropy are derived from the calculated vibrational spectrum within the quasi-harmonic approximation.

II. METHOD

Computations are performed using the density functional perturbation theory (DFPT) (Ref. 18) within the local density approximation.[20] Mg pseudopotential is generated by the method of von Barth and Car.[21] In this scheme a simple analytic form for the pseudopotential is assumed whose parameters are determined by minimizing the squared differences of pseudo and all-electron wave functions for a number of configurations. Five configurations $3s^2 3p^0$, $3s^1 3p^1$, $3s^1 3p^{0.5} 3d^{0.5}$, $3s^1 3p^{0.5}$, and $3s^1 3d^1$ with decreasing weights 1.5, 0.6, 0.3, 0.3, and 0.2 respectively, are used. The core radii are $r(3s)=2.4$ a.u.; $r(3p)=3.0$ a.u.; $r(3d)=3.5$ a.u. with d local. The O pseudopotential is generated using the method of Troullier and Martin[22] from the configuration $2s^2 2p^4$ with core radii $r(2s)=1.45$ a.u., and $r(2p)=1.45$ a.u., and with p locality. A plane wave basis set with cutoff of 90 Ry is used to expand the valence electronic wave functions. Brillouin zone summations of electronic quantities are performed over 6 special k points for the equilibrium struc-

ture, and larger numbers of equivalent points for the deformed lattices.

Frequencies $\omega(\mathbf{q})$ and polarization vectors $\mathbf{u}_\kappa(\mathbf{q})$ of phonons with wave vectors $\mathbf{q}$ are determined by the diagonalisation of the dynamical matrix

$$D^{\alpha\beta}_{\kappa\kappa'}(\mathbf{q}) = \frac{1}{\sqrt{m_\kappa m_{\kappa'}}} \sum_l \Phi^{\alpha\beta}_{\kappa\kappa'}(0\ l)\exp[-i\mathbf{q}\cdot(\mathbf{x}_0 - \mathbf{x}_l)]$$

which satisfies the eigenvalue problem

$$\sum_{\kappa'} D_{\kappa\kappa'}(\mathbf{q})\mathbf{u}_{\kappa'}(\mathbf{q}) = \omega^2(\mathbf{q})\mathbf{u}_\kappa(\mathbf{q}).$$

Here an infinite crystal is divided up into primitive cells (labeled by l) each containing r atoms (labeled by κ) with ionic mass m_κ. The real space interatomic force constants $\Phi^{\alpha\beta}_{\kappa\kappa'}(0\ l)$ include ionic and electronic contributions, so

$$\Phi^{\alpha\beta}_{\kappa\kappa'}(0\ l) = \Phi^{\alpha\beta}_{\kappa\kappa'}(0\ l)_{ion} + \Phi^{\alpha\beta}_{\kappa\kappa'}(0\ l)_{el}.$$

The ionic contribution can be calculated from Ewald sums. The electronic contribution can be expressed as

$$\Phi^{\alpha\beta}_{\kappa\kappa'}(0\ l)_{el} = \int \left[\frac{\partial\rho(\mathbf{r})}{\partial u^\alpha_\kappa(0)} \frac{\partial V_{ion}(\mathbf{r})}{\partial u^\beta_{\kappa'}(l)} \right. \\ \left. + \rho(\mathbf{r}) \frac{\partial^2 V_{ion}(\mathbf{r})}{\partial u^\alpha_\kappa(0)\partial u^\beta_{\kappa'}(l)} \right] d^3r,$$

where $\rho(\mathbf{r})$ is the electron density, $V_{ion}(\mathbf{r})$ is the ionic potential, and $\partial\rho(\mathbf{r})/\partial u^\alpha_\kappa(0)$ represents the density response of the system to a displacement of the κ atom in the reference cell ($l=0$) along the α direction. This linear electron-density response can be calculated self-consistently using DFPT. It is convenient to treat lattice displacements with a given periodicity $\mathbf{q}$, $u^\alpha_\kappa(l) = \tilde{u}^\alpha_\kappa(\mathbf{q})\exp[i\mathbf{q}\cdot\mathbf{x}_l]$, since the corresponding linear density response has the same periodicity and the dynamical matrix $D^{\alpha\beta}_{\kappa\kappa'}(\mathbf{q})$ and the corresponding phonons can be determined directly at any wavevector $\mathbf{q}$ in the BZ without need of supercells.

Since MgO is a polar compound, the macroscopic electric field caused by the long-range character of the Coulomb forces contributes to the LO phonon in the long-wavelength ($\mathbf{q}\to 0$) limit. This effect is included by calculating the nonanalytical behavior of the force constants as given by

$$\frac{4\pi e^2}{V} \frac{(\mathbf{q}\cdot\mathbf{Z}^*_\kappa)_\alpha (\mathbf{q}\cdot\mathbf{Z}^*_{\kappa'})_\beta}{\mathbf{q}\cdot\epsilon_\infty\cdot\mathbf{q}},$$

where tensors $\mathbf{Z}^*$ and ϵ_∞ are, respectively, the Born effective charges and the macroscopic high-frequency static dielectric constant which are also calculated self-consistently using DFPT.

III. RESULTS AND DISCUSSION

A. Static lattice

We first determine the equilibrium volume of MgO by calculating the total energy per primitive cell as a function of volume. A fourth-order finite strain equation[23] fit to the cal-
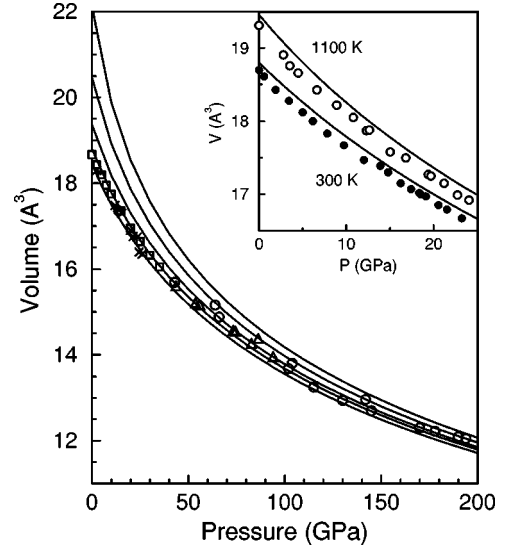
FIG. 1. Pressure-volume equations of state for the static lattice and at 300, 1000, 2000, and 3000 K isotherms (lines from bottom to top). The experimental data at room temperature are denoted by squares (Ref. 9), crosses (Ref. 10), triangles (Ref. 11) and circles (Ref. 1). The inset shows comparison with the data (symbols) obtained under hydrostatic conditions (Ref. 24).

culated energy-volume results yields $V_0 = 18.48$ Å^3, $K_0 = 169$ GPa, $K'_0 = 4.18$, and $K''_0 = -0.025$ GPa^{-1}. The predicted pressure-volume results compare well with the room temperature experimental data[1,9–11] over a wide pressure regime (Fig. 1). The agreement with experiments improves further when the zero-point motion and finite temperature corrections are included, as we show later.

B. Lattice dynamics

MgO exists in the rock-salt structure (space group $Fm3m$). The vibrational frequencies of MgO are determined at several volumes (or pressures) within the linear response framework. Dynamical matrices are computed at eight wave ($\mathbf{q}$) vectors in the irreducible wedge of BZ, i.e., on $4\times 4\times 4$ $\mathbf{q}$ grid, and are used for interpolation to obtain the bulk phonon dispersions. The predicted dispersion curves along several symmetry directions at zero and 100 GPa are shown in Fig. 2. The phonon frequencies at high-symmetry points Γ, X, and L are also given in Table I. Our results at zero pressure conditions are in agreement with the neutron-scattering data at ambient condition,[12] and with previous *ab initio* results.[17]

The volume dependence of the frequencies can be expressed by the mode Grüneisen parameters

$$\gamma_i = -d\ln\omega_i/d\ln V.$$

Dispersion curves for mode Grüneisen parameters at zero pressure are shown in Fig. 3. The acoustic mode Grüneisen parameters in the limit of $\mathbf{q}\to 0$ depend on the direction the zone center is approached from and hence they show discontinuities at Γ. The values of six vibrational modes measured in the sideband spectra of MgO:Cr^{3+} ranges from 0.98 to 1.69 from Ref. 13. Our study provides upper and lower bounds on the value of γ_i's, which are 0.4 and 2.8, respec-
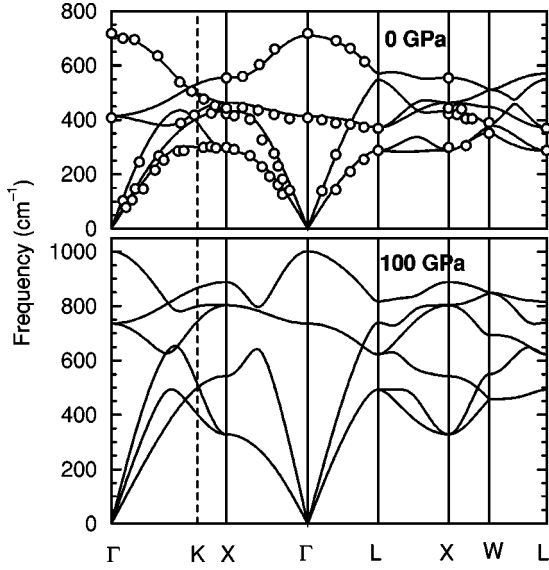
FIG. 2. Phonon dispersions at 0 and 100 GPa. Symbols are experimental data at ambient condition (Ref. 12).

tively, at zero pressure and 0.3 and 1.7, respectively, at 100 GPa. The mode Grüneisen parameters are found to be positive throughout the BZ for all branches (Fig. 3) suggesting that none of the modes soften with compression and MgO is dynamically stable. The pressure dependence of Γ, X and L phonons is nearly linear at high pressures (Fig. 4). The LO-TO splitting at Γ remains nearly unchanged with compression. A similar trend is shown by L modes but the splitting increases rapidly with pressure at X.

The calculated value of the static high-frequency dielectric constant constant (ϵ_∞) is 3.10 compared to the experimental value of 2.94 at ambient condition. As pressure rises, ϵ_∞ decreases monotonically to 2.8 at 150 GPa. Our results show that the Born effective charges (± 1.93 for Mg and O ions) at zero pressure are close to formal ionic value of 2 but decrease slightly with increasing pressure (± 1.77 at 150 GPa).

C. Thermoelastic properties

In the quasiharmonic approximation (QHA), the Helmholtz free energy is given by

$$F(V,T) = U_0(V) + \frac{1}{2} \sum_{\mathbf{q},j} h\omega_j(\mathbf{q},V)$$

$$+ k_B T \sum_{\mathbf{q},j} \ln\{1 - \exp[-h\omega_j(\mathbf{q},V)/k_B T]\},$$

TABLE I. Calculated zero pressure phonon frequencies (in cm^{-1}) of MgO at Γ, X, and L compared with experiments (Ref. 12) and previous calculations (Ref. 17).

	Γ_{TO}	Γ_{LO}	X_{TA}	X_{LA}	X_{TO}	X_{LO}	L_{TA}	L_{LA}	L_{TO}	L_{LO}
This study	414	710	289	433	464	555	287	548	371	570
Prev Cal	391	709	288	420	446	552	274	547	357	569
Exp	408	718	299	422	443	554	288		369	
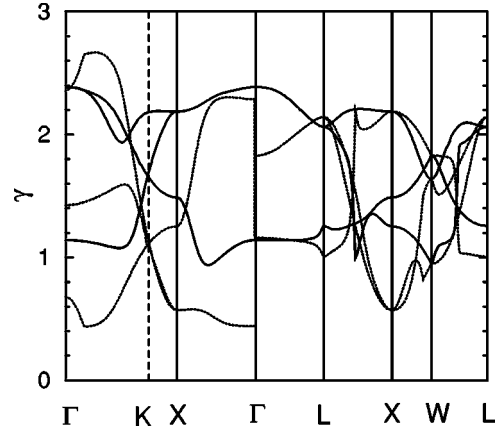
FIG. 3. Mode Grüneisen parameters at zero pressure. The dotted lines represent acoustic modes.

where the first, second, and third terms are, respectively, the internal, zero point, and vibrational contributions. The summation is performed on a $12 \times 12 \times 12$ regular $\mathbf{q}$ mesh including 1728 points in the first BZ that are found to be sufficient for convergence. At the level of the QHA, frequencies depend on volume while intrinsic anharmonic effects arising from phonon-phonon interaction are neglected. The latter increases with temperature and the QHA becomes increasingly less adequate at high temperatures. On the other hand, anharmonic effects become less important with increasing pressure. With decreasing volume the leading harmonic term in the expansion of the potential energy in terms of atomic displacements is expected to become increasingly predominant, so the QHA generally works well over a wider temperature range at elevated pressures.

1. Equation of state

Isothermal fourth-order finite strain equations[23] are used to obtain functional forms for the calculated Helmholtz free energy versus volume. The resulting pressure-volume equation of state (EOS) isotherms are shown in Fig. 1. The 300 K isotherm lies slightly above the static result and agrees fairly
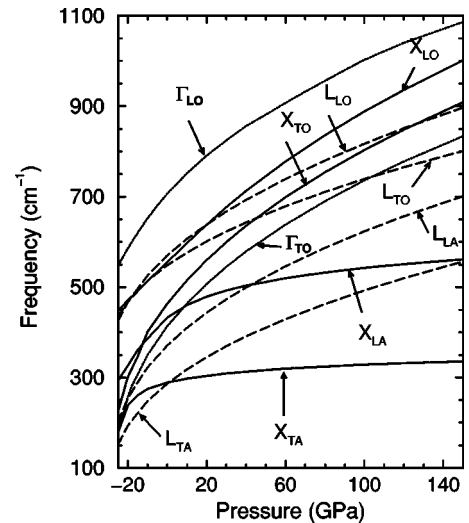
FIG. 4. Pressure dependence of the frequencies of high symmetry phonons (Γ, X, and L).

TABLE II. Calculated thermodynamic parameters of MgO at ambient conditions, compared with experiments and previous calculations.

	V Å^3	K_T GPa	K_T'	K_T'' GPa^{-1}	(dK_T/dT) GPa K^{-1}	$\alpha \times 10^{-5}$ K^{-1}	γ_{th}	C_P $\text{J mol}^{-1}\text{K}^{-1}$	S $\text{J mol}^{-1}\text{K}^{-1}$
This Study	18.81	159	4.30	-0.030	-0.0266	3.10	1.542	37.06	26.65
VIB (Ref. 7)	18.70	153	4.68	-0.05		3.88	~ 1.4		
PIB (Ref. 5)	18.66	180	4.15	-0.026		2.39	1.45		
Exp. (Refs. 16,24,25)	18.69	160(2)	4.15		-0.027	3.12(16)	1.54(8)	37.67	

well with the observed data.[1,9–11] The calculated EOS parameters of MgO at ambient conditions are shown in Table II. The effects of the zero point motion and room temperature are to increase V_0 (volume) by $\sim 2\%$ and decrease K_{T0} (isothermal bulk modulus) by $\sim 6\%$ from their athermal values given by the static calculations. The calculated parameters are found to be in agreement with observed experimental data obtained under hydrostatic conditions.[24] Similarly, our results at 1100 K of $V_0 = 19.44$ Å^3, $K_{T0} = 136$ GPa, and $K_{T0}' = 4.48$ ($K_{T0}'' = -0.039$ GPa^{-1}) compare well with the experimental data[24] of 19.31 Å^3, 135(3) GPa, and 4.20.

The value of our calculated thermal expansivity

$$\alpha = \frac{1}{V}\left[\frac{\partial V}{\partial T}\right]_P$$

is 3.11×10^{-5} K^{-1} at zero pressure and 300 K in agreement with the measured value[25] of 3.12×10^{-5} K^{-1}. As temperature rises, α is found to increase relatively rapidly compared to the experimental data[25] (Fig. 5); the difference between theory and experiment is 7% at 1000 K whereas it exceeds 25% at 2000 K. Beyond 1000 K or so, the deviation increases rapidly as T approaches the melting point (~ 3000 K for MgO). Similar behavior was predicted by previous calculations based on the potential induced breathing (PIB)

model.[5] This is an indication of the inadequacy of the QHA at high temperatures and low pressures. As shown by molecular dynamics simulations based on variational induced breathing (VIB) model,[7] the inclusion of anharmonic effects tends to give rather slow and linear high temperature dependence of α at zero pressure. With increasing pressure, α decreases rapidly, and the effects of temperature become less and less pronounced resulting in linear high temperature behavior. Our results show that α converges to a constant value at high temperatures and high pressures. The calculated value compares well with the average value of α between 300 and ~ 3300 K in the pressure range of 169 to 196 GPa obtained from the shock-wave experiments.[26]

The thermal Grüneisen parameter which is useful in reducing high-temperature equation of state in shock-compression experiments is defined as

$$\gamma_{\text{th}} = \frac{V\alpha K_T}{C_V},$$

where C_V is the heat capacity at constant volume. It is also a useful indicator for the importance of anharmonicity, increasing with the latter. At zero pressure, the calculated γ_{th} increases monotonically with temperature from its room temperature value of 1.54 whereas experiments[16] have found that γ_{th} remains nearly constant at 1.52 (Fig. 6). As in the
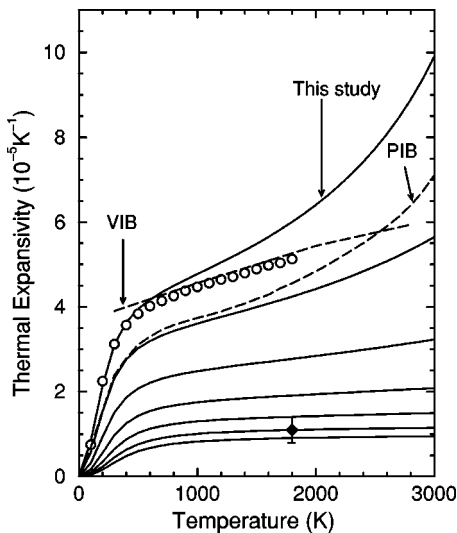
FIG. 5. Pressure and temperature dependence of thermal expansivity. The isobars at 0, 10, 30, 60, 100, 150, and 200 GPa are represented by solid lines from top to bottom. Experimental data at ambient pressure are denoted by circles (Ref. 25) and those at 169–196 GPa by diamond (Ref. 26). Dashed lines are PIB (Ref. 5) and VIB (Ref. 7) calculations at zero pressure.
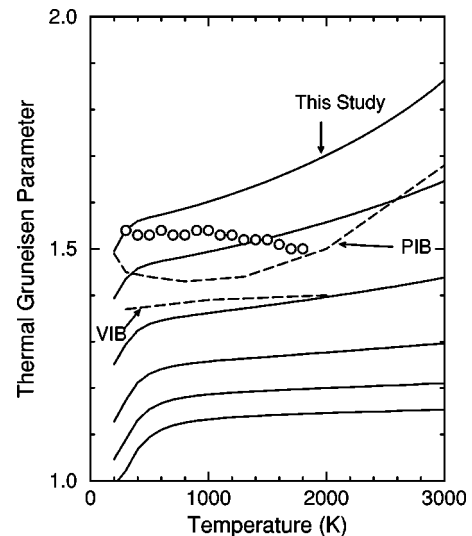
FIG. 6. Pressure and temperature dependence of thermal Grüneisen parameter. The isobars at 0, 10, 30, 60, 100, and 150 GPa are represented by solid lines from top to bottom. Experimental data at ambient pressure are denoted by circles Ref. 16. Dashed lines are PIB (Ref. 5) and VIB (Ref. 7) calculations at zero pressure.
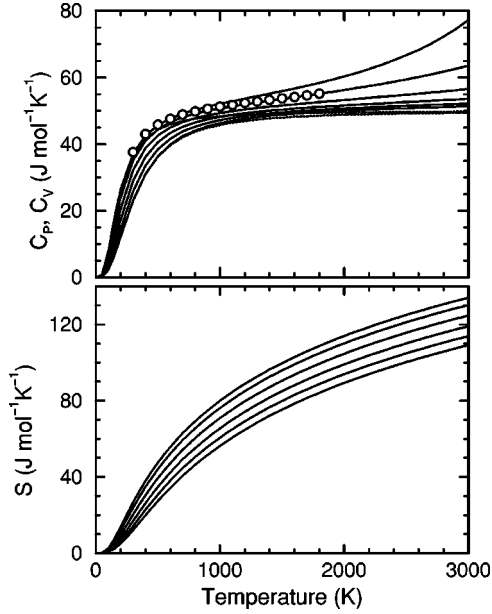
FIG. 7. Pressure and temperature dependence of heat capacity and entropy. The isobars at 0, 10, 30, 60, 100, and 150 GPa are represented by solid lines from top to bottom. Experimental data at ambient pressure are denoted by symbols (see, Ref. 16). Dotted lines represent the constant volume specific heat at 0 and 150 GPa.

case of thermal expansivity, strong temperature dependence of γ_{th} at low pressure is attributed to the QHA. However, at higher pressures, γ_{th} is found to be nearly independent of temperature. The volume dependence of γ_{th} is usually expressed by a parameter $q = (\partial \ln \gamma_{th} / \partial \ln V)_T$. We find that at zero pressure, q decreases from 1.39 to 1.2 from 300 to 1000 K, and then increases to 1.32 at 3000 K. At all temperatures, the calculated value of q rapidly decreases with increasing pressure. The calculated value at 150 GPa is 0.65 at 300 K and ~ 0.5 at higher temperatures.

Heat capacity and entropy are calculated from phonon frequencies within the QHA (Fig. 7). The heat capacity at constant pressure (C_P) is given by $C_P = C_V(1 + \alpha \gamma_{th} T)$ so the difference in C_V and C_P gives a measure of lattice anharmonicity. The calculated values of C_V and C_P at ambient condition are 36.53 and 37.06 J mol^{-1} K^{-1}, respectively, compared to the experimental value[16] of $C_P = 37.67$ J mol^{-1} K^{-1}. At zero pressure, with increasing temperature beyond 1000 K, C_P deviates rapidly from C_V and the experimental value, indicating the failure of QHA. But at high pressure, C_P shows a slight linear increase with temperature remaining close to C_V at all temperatures. The entropy is shown to be 26.65 J mol^{-1} K^{-1} at ambient condition. Unlike α, γ_{th} and C_P, the high temperature dependence of entropy is nearly insensitive to pressure.

2. Elastic moduli

The isothermal bulk modulus K_T is related to the adiabatic bulk modulus K_S by $K_S = K_T(1 + \alpha \gamma_{th} T)$. The fitting EOS parameters are used to calculate K_T and hence K_S as a function of pressure and temperature. With $K_S = (c_{11} + 2c_{12})/3$, two independent adiabatic elastic constants c_{11} and c_{12} are determined by calculating $c_s = c_{11} - c_{12}$. At a given volume, the unit cell is distorted with tetragonal strain

$$\epsilon_{te} = \begin{pmatrix} 2e & 0 & 0 \\ 0 & -e & 0 \\ 0 & 0 & -e \end{pmatrix}$$

to determine c_s from the free energy density to second order in e using

$$F_{te} = 3c_s e^2.$$

The shear elastic constant c_{44} is obtained by applying shear strain

$$\epsilon_{sh} = \begin{pmatrix} 0 & e & e \\ e & 0 & e \\ e & e & 0 \end{pmatrix}$$

for which the free energy density to second order in e is

$$F_{sh} = 6c_{44} e^2.$$

Note that the above strains conserve volume only to first order in e so corrections for the second order change in volume are included into the free energy density. Different magnitudes ($e = 0.01$, 0.02, and 0.03) of the strain are used to determine c_s in the limit of zero strain. However, the single value of $e = 0.02$ is used in the case of c_{44} as its value is found to be insensitive to the magnitude of the strain used. We study the temperature dependence of c_s and c_{44} for which the adiabatic and isothermal values are equal by calculating the quasiharmonic free energies from the phonon dispersions of the strained lattices at several volumes. In other words, it requires the calculation of strain dependence of the free energy at the volume corresponding to a given temperature and pressure. Our calculated free energies and elastic moduli thus include contributions from volume and strain dependent phonon frequencies.

The predicted zero pressure elastic moduli of MgO for static lattice and at 300 K are shown in Table III. Our results are in agreement with the measured data at ambient conditions.[15] The zero point motion and 300 K effects are relatively large for c_{11}, compared to c_{12} and c_{44}, decreasing the values of c_{11} and c_{44} by 8 and 3 %, respectively, but increasing the value of c_{12} by 1%. The overall agreement with measurements is substantially better than previous calculations. In particular, previous pseudopotential calculations[8] appear to underestimate the elastic moduli (largely if zero point and 300 K temperature corrections are taken into account) as it has also overestimated the volume, whereas PIB results[5] are substantially overestimated (Table III).

Our calculated elastic moduli at zero pressure, in general, agree well with experimental data[16,27] over a wide temperature range (Fig. 8). However, the calculations appear to increasingly deviate from the experimental trend at temperatures roughly above 1000 K where the QHA approximation is shown to overestimate the thermal expansion significantly. The predicted results for initial pressure dependencies of the elastic moduli at room temperature also compare fairly well with the available low pressure data (Fig. 9) from Refs. 15,28.

The temperature dependence is shown to be sensitive to pressure to different extents for different elastic constants
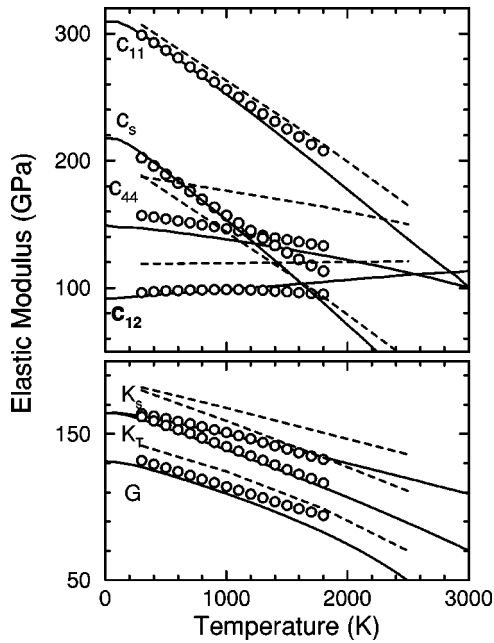
FIG. 8. Calculated temperature dependence of elastic moduli at zero pressure (solid lines), compared to experimental data (Ref. 16) denoted by circles, and PIB calculations (Ref. 5) denoted by dashed lines.

(Fig. 9). The calculated isotherms are nearly parallel throughout the pressure range studied in c_{11} whereas the isotherms tend to converge at low pressures but remain nearly parallel at high pressures in c_{44}. The temperature shift in c_{12} shows slight nonmonotonical trend with pressure; the temperature-induced increase in c_{12} at first falls slightly up to 20 GPa and then rises at higher pressures. Our predicted cross pressure-temperature variations of the elastic moduli
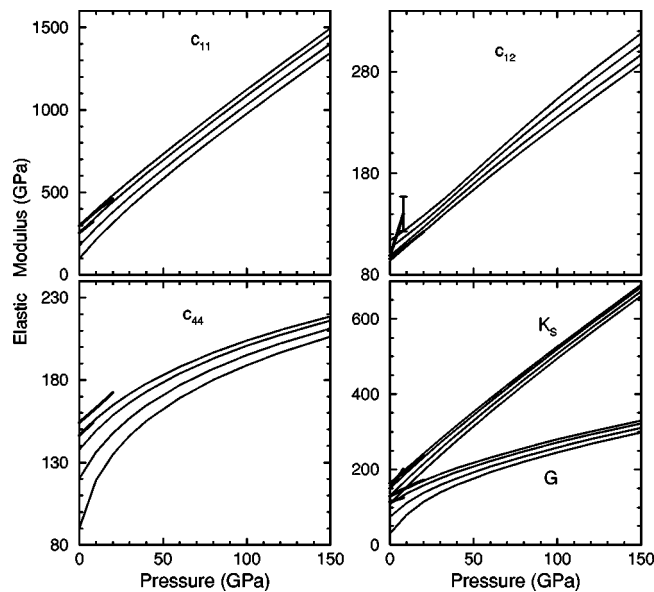
disagree with recent cross P-T experimental data (to 8 GPa and 1600 K).[14] The calculated mixed P-T derivatives at ambient conditions ($\partial^2 c_{ij}/\partial P \partial T$) are much smaller in the magnitude and opposite in the sign compared to the observed values[14] (Table III). However, our results are comparable to the earlier data[29] from the experiments to 800 K and 0.8 GPa, and also to those predicted by the PIB model calculations.[5] In particular, we find that the cross derivative of c_{12} is small and negative (-0.06×10^{-3} K^{-1}) at 0 GPa but it becomes positive beyond 20 GPa and slightly increases in magnitude, whereas the value of 5.1×10^{-3} K^{-1} in Ref. 14 is relatively large in magnitude. Accordingly, the measured cross derivative value for bulk modulus (K_S) is large and positive (about 3.0×10^{-3} K^{-1}) but that for shear modulus (G) is large and negative (about -1.8×10^{-3} K^{-1}) (Table III). With raising temperature from 300 to 1000 K, measured K_S decreases from its room temperature value by $\sim 8\%$ at zero pressure but K_S increases with temperature at pressures above 6 GPa. The sizes of temperature-induced decrease in G are ~ 13 and $\sim 17\%$, respectively, at 0 and 6 GPa. Thus the measured cross derivative value of the bulk modulus appears to be very large, and is indeed the largest ever reported value.[30] Our predicted cross derivatives are instead relatively small and positive so temperature-induced variations in both bulk and shear moduli are monotonically suppressed by pressure. The calculated isotherms converge (more rapidly in shear than bulk moduli) with increasing pressure becoming nearly parallel at very high pressures (Fig. 9).

While the uncertainties in the experiments are significant, the reason for the discrepancy between theory and latest measured data[14] is unknown. That our calculations reproduced well the measured pressure dependencies of the elastic moduli at ambient temperature and the measured temperature dependence at ambient pressure suggests that the predicted cross P-T variations of the elastic moduli should also be equally accurate. This is further substantiated by the fact that the QHA should work even better at higher pressures. It is important to note that unlike first-order pressure or temperature derivatives, the cross P-T derivatives are difficult to constrain in the experiments and are likely to be sensitive to the P-T range studied.

IV. CONCLUSIONS

The vibrational spectrum of MgO has been investigated up to 150 GPa using density functional perturbation theory and several thermodynamical quantities of interest have been derived within the quasi-harmonic approximation (QHA). The calculated mode Grüneisen parameters span the range of 0.4 to 2.8 at zero GPa and 0.3 to 1.7 at 100 GPa indicating the dynamical stability of the rock-salt structure over a wide pressure range. Pressure dependencies of the frequencies are shown to be linear at high pressure. By calculating the free energies from phonon dispersions of equilibrium and strained lattices within the QHA, several physical quantities of interest are determined as a function of temperature and pressure. At zero pressure, the temperature dependence of thermal expansivity, thermal Grüneisen parameter, and constant pressure heat capacity is found to be in agreement with the experimental results at low temperatures but the

FIG. 9. Pressure variation of elastic Moduli along 300, 1000, 2000, and 3000 K isotherms (solid lines from top to bottom for c_{11}, c_{44}, K_S, and G, and those from bottom to top for c_{12}). Thick lines are low pressure experimental data at 300 (Ref. 15) and 1000 K (Ref. 14).

TABLE III. Calculated pressure and temperature derivatives (from fourth order polynomial fits) of elastic moduli of MgO compared to experiments and other calculations.

		This Study	Exp. (Refs. 14–16,29)	PIB (Ref. 5)	PWPP[a] (Ref. 8)
	c_{11}	300, 323 [a]	297.9(15)	308	290
	c_{12}	93.6, 92 [a]	95.8(10)	119	92
M	c_{44}	147, 152 [a]	154.4(20)	188	138
(GPa)	K_S	162.4, 169 [a]	163.2(10)	182	158
	G	127.6, 135 [a]	130.2(10)	143	121
	c_{11}	9.56	9.05(20)	8.20	9.16
	c_{12}	1.45	1.34(15)	2.08	1.64
$\partial M/\partial P$	c_{44}	1.03	0.84(20)	0.95	0.81
	K_S	4.15	4.0(1)	4.12	4.15
	G	2.44	2.4(1)		2.37
	c_{11}	-0.0598	-0.0585	-0.053	
	c_{12}	0.0089	0.0075	0.002	
$\partial M/\partial T$	c_{44}	-0.0088	-0.0126	-0.012	
(GPa K^{-1})	K_S	-0.0140	-0.0145	-0.016	
	G	-0.0216	-0.024		
	c_{11}	0.56	$-1.3(4),0.1(4)$	0.52	
	c_{12}	-0.06	5.1(24),0.1(3)	0.03	
$\partial^2 M/\partial P\partial T$	c_{44}	0.20	$-0.2(3),0.1(1)$	0.25	
($\times10^{-3}$K^{-1})	K_S	0.14	3.0(15),0.1(3)	0.19	
	G	0.44	$-1.8(10),0.1(2)$		

[a]For the static lattice.

predicted behavior starts to deviate from the experimentally observed linear trend beyond ~ 1000 K. It is shown that with increasing pressure, temperature effects are suppressed resulting in a linear high temperature behavior. Each of these quantities is shown to converge to a nearly constant value at high pressure and temperature. Similarly, the experimentally determined ambient values and initial pressure (at 300 K) and temperature (at 0 GPa) dependencies of elastic moduli are reproduced well by our calculations. The contributions from zero point motion and 300 K to the elastic moduli are shown to be significant ($\sim 8\%$ in c_{11} and $\sim 6\%$ in bulk modulus), therefore, one should be careful in comparing the athermal (static) results with the ambient experimental data. Our predicted cross pressure-temperature derivatives of c_{ij}'s are considerably smaller (with opposite sign) than those obtained in the latest experiments[14] to 8 GPa and 1600 K, however, they are consistent with those obtained in earlier experiments.[29] In particular, we notice that the value of cross derivative of c_{12} as implied by the latest experiments is unusually large, resulting in a sharp contrast in cross P-T variations of isotropic bulk and shear moduli.

Elasticity at high pressures and temperatures is a particularly significant topic to Earth sciences. The pressure-temperature range pertinent to the Earth's mantle (P up to 135 GPa, T up to 3000 K) is very challenging for experiments. Here we demonstrate that the QHA combined with first principles phonon calculations successfully describes thermoelastic properties of MgO, an important Earth forming mineral, within the pertinent pressure-temperature range. This potentially represents an important approach for exploring materials properties over a considerable temperature range at elevated pressure, especially Earth forming phases within the geothermal profile.

*Also at Instituto Nazionale Fisica della Materia (INFM), I-34014 Trieste, Italy.

[1] T. H. Duffy, R. J. Hemely, and H. K. Mao, Phys. Rev. Lett. **74**, 1371 (1995).

[2] K. J. Chang and M. L. Cohen, Phys. Rev. B **30**, 4774 (1984).

[3] M. S. T. Bukowinski, Geophys. Res. Lett. **12**, 536 (1985).

[4] M. J. Mehl, R. E. Cohen, and H. Krakauer, J. Geophys. Res. **93**, 8009 (1988).

[5] D. G. Isaak, R. E. Cohen, and M. E. Mehl, J. Geophys. Res. **95**, 7055 (1990).

[6] H. Zhang and M. S. T. Bukowinski, Phys. Rev. B **44**, 2495 (1991).

[7] I. Inbar and R. E. Cohen, Geophys. Res. Lett. **22**, 1533 (1995).

[8] B. B. Karki, L. Stixrude, S. J. Clark, M. C. Warren, G. J. Ackland, and J. Crain, Am. Mineral. **82**, 51 (1997).

[9] E. A. Perez-Albuerne and H. G. Drickamer, J. Chem. Phys. **43**, 1381 (1965).

[10] J. S. Weaver, T. Takahashi, and W. A. Bassett, in *Accurate Characterization of the High Pressure Environment*, edited by E. C. Lloyd (NBS, Washington, D.C., 1971), p. 189.

[11] H. K. Mao and P. M. Bell, J. Geophys. Res. **84**, 4533 (1979).

[12] M. J. L. Sangster, G. Peckham, and D. H. Saunderson, J. Phys. C **3**, 1026 (1970).

[13] A. Chopelas, Epilepsia Phys. Earth Plant Inter **98**, 3 (1996).

[14] G. Chen, R. C. Liebermann, and D. J. Weidner, Science **280**, 1913 (1998).

[15] S. V. Sinogeikin and J. D. Bass, Phys. Rev. B **59**, 14 141 (1999).

[16] D. G. Isaak, O. L. Anderson, and T. Goto, Phys. Chem. Miner. **16**, 704 (1989).

[17] O. Schütt, P. Pavone, W. Windl, K. Karch, and D. Strauch, Phys. Rev. B **50**, 3746 (1994).

[18] S. Baroni, P. Giannozzi, and A. Testa, Phys. Rev. Lett. **58**, 1861 (1987); P. Giannozzi, S. de Gironcoli, P. Pavone, and S. Baroni, Phys. Rev. B **43**, 7231 (1991).

[19] B. B. Karki, R. M. Wentzcovitch, S. de Gironcoli, and S. Baroni, Science **286**, 1705 (1999).

[20] J. P. Perdew and A. Zunger, Phys. Rev. B **23**, 5048 (1981).

[21] U. von Barth and R. Car (unpublished).

[22] N. Troullier and J. L. Martins, Phys. Rev. B **43**, 1993 (1991).

[23] F. D. Birch, J. Geophys. Res. **91**, 4949 (1986).

[24] Y. Fei, Am. Mineral. **84**, 272 (1999).

[25] Y. S. Touloukian, R. K. Kirdby, R. E. Taylor, and T. Y. R. Lee, *Thermophysical Properties of Matter* (Plenum, New York, 1977), Vol. 13.

[26] T. S. Duffy and T. Ahrens, Geophys. Res. Lett. **20**, 1103 (1993).

[27] Y. Sumino, O. L. Anderson, and I. Suzuki, Phys. Chem. Miner. **9**, 38 (1983).

[28] I. Jackson and H. Niesler, in *High Pressure Research in Geophysics*, edited by S. Akimoto and M. H. Manghnani (Center for Academic Publications Japan, Tokyo, 1982), p. 93.

[29] H. A. Spetzler, J. Geophys. Res. **75**, 2073 (1970).

[30] D. G. Isaak and E. K. Graham, J. Geophys. Res. **81**, 2483 (1976); G. Chen, A. Yoneda, I. C. Getting, and H. A. Spetzler, *ibid.* **101**, 25 161 (1996).